# SANDIA REPORT

SAND2013-2609
Unlimited Release
Printed March 2013

# Development and Deployment of Constitutive Softening Routines in Eulerian Hydrocodes

Timothy J. Fuller, Tom Dewers, M. Scot Swan

Prepared by
Sandia National Laboratories
Albuquerque, New Mexico 87185 and Livermore, California 94550

Sandia is a multi-program laboratory operated by Sandia Corporation,
a wholly owned subsidiary of Lockheed Martin Corporation, for the United States Department
of Energy's National Nuclear Security Administration under Contract DE-AC04-94AL85000.

Approved for public release; further dissemination unlimited.

Sandia National Laboratories

Issued by Sandia National Laboratories, operated for the United States Department of Energy by Sandia Corporation.

**NOTICE:** This report was prepared as an account of work sponsored by an agency of the United States Government. Neither the United States Government, nor any agency thereof, nor any of their employees, nor any of their contractors, subcontractors, or their employees, make any warranty, express or implied, or assume any legal liability or responsibility for the accuracy, completeness, or usefulness of any information, apparatus, product, or process disclosed, or represent that its use would not infringe privately owned rights. Reference herein to any specific commercial product, process, or service by trade name, trademark, manufacturer, or otherwise, does not necessarily constitute or imply its endorsement, recommendation, or favoring by the United States Government, any agency thereof, or any of their contractors or subcontractors. The views and opinions expressed herein do not necessarily state or reflect those of the United States Government, any agency thereof, or any of their contractors.

Printed in the United States of America. This report has been reproduced directly from the best available copy.

Available to DOE and DOE contractors from
U.S. Department of Energy
Office of Scientific and Technical Information
P.O. Box 62
Oak Ridge, TN 37831

Telephone: (865) 576-8401
Facsimile: (865) 576-5728
E-Mail: reports@adonis.osti.gov
Online ordering: http://www.osti.gov/bridge

Available to the public from
U.S. Department of Commerce
National Technical Information Service
5285 Port Royal Rd
Springfield, VA 22161

Telephone: (800) 553-6847
Facsimile: (703) 605-6900
E-Mail: orders@ntis.fedworld.gov
Online ordering: http://www.ntis.gov/help/ordermethods.asp?loc=7-4-0#online

SAND2013-2609
Unlimited Release
Printed March 2013

# Development and Deployment of Constitutive Softening Routines in Eulerian Hydrocodes

Timothy J. Fuller
Computational Structural Mechanics and Applications
Sandia National Laboratories
P.O. Box 5800
Albuquerque, NM 87185-0840 tjfulle@sandia.gov

Tom Dewers
Geomechanics
Sandia National Laboratories
P.O. Box 5800
Albuquerque, NM 87185-0751
tdewers@sandia.gov

M. Scot Swan
Sandia National Laboratories
P.O. Box 5800
Albuquerque, NM 87185-1323
mswan@sandia.gov

**Abstract**

The state of the art in failure modeling enables assessment of crack nucleation, propagation, and progression to fragmentation due to high velocity impact. Vulnerability assessments suggest a need to track material behavior through failure, to the point of fragmentation and beyond. This field of research is particularly challenging for structures made of porous quasi-brittle materials, such as ceramics used in modern armor systems, due to the complex material response when loading exceeds the quasi-brittle material's elastic limit. Further complications arise when incorporating the quasi-brittle material response in multi-material Eulerian hydrocode simulations.

In this report, recent efforts in coupling a ceramic materials response in the post-failure regime with an Eulerian hydro code are described. Material behavior is modeled by the Kayenta material model [2] and ALEGRA as the host finite element code [14]. Kayenta, a three invariant phenomenological plasticity model originally developed for modeling the stress response of geologic materials, has in recent years been used with some success in the modeling of ceramic and other quasi-brittle materials to high velocity impact. Due to the granular nature of ceramic materials, Kayenta allows for significant pressures to develop due to dilatant plastic flow, even in shear dominated loading where traditional equations of state predict little or no pressure response. When a material's ability to carry further load is compromised, Kayenta allows the material's strength and stiffness to progressively degrade through the evolution of damage to the point of material failure. As material dilatation and damage progress, accommodations are made within ALEGRA to treat in a consistent manner the evolving state.

# Acknowledgment

The first author would like to thank the mentorship and assistance of Tom Dewers and Mike Wong of SNL and Rebecca Brannon of the University of Utah during the course of this project. Also Scot Swan (SNL) for the long discussions and assistance in developing the constitutive softening routines used throughout this project.

# Contents


**1 Introduction** **13**

**2 The Kayenta Material Model** **15**

2.1 Elasticity . . . . . 15

2.2 Plastic Flow . . . . . 16

2.2.1 Isochoric Plastic Flow . . . . . 16

2.2.2 Dilatant Plastic Flow . . . . . 17

2.3 The Kayenta Limit Surface . . . . . 17

2.4 Elastic-Plastic Coupling . . . . . 19

2.4.1 Form of the $z$ Tensor . . . . . 19

2.5 Magnitude of the Plastic Strain Rate: The Consistency Condition . . . . . 20

2.5.1 Some Effects of Elastic-Plastic Coupling . . . . . 20

2.6 Softening . . . . . 20

**3 Response of Quasi-brittle Materials in Shock-Hydrocode Simulations** **27**

3.1 Coupling the Response of Kayenta with an Equation of State . . . . . 27

3.2 Tensile Control in Shock-Hydrocode Simulations . . . . . 28

3.3 Comparison of Density with/without Tensile Control . . . . . 30

3.4 Application of Kayenta to Penetration Predictions in Ceramic Armor Systems 30

3.5 Conclusion . . . . . 31

**4 Payette, An Object Oriented Material Model Driver** **33**

4.1 Introduction . . . . . 33

4.2 Why a Single Point Material Driver? . . . . . 33
4.3 Obtaining and Building Payette . . . . . 34
4.4 Payette: Key Features . . . . . 34
4.4.1 User Interaction . . . . . 34
4.4.1.1 Payette Input File Format . . . . . 34
4.4.1.2 Payette Graphical User Interface . . . . . 35
4.4.2 Visualization of Constitutive Model Data . . . . . 36
4.4.3 Parameter Sensitivity and Optimization . . . . . 36
4.4.3.1 The `permutation` Block . . . . . 37
4.4.3.2 The `optimization` Block . . . . . 38
4.5 Conclusion . . . . . 38

**5 Conclusion** **41**

# List of Figures


2.1 Deviatoric return direction results in isochoric plastic flow for the Von Mises yield criterion. The $x$-axes variable $\bar{I}_1$ is the *negative* of the first invariant of the stress tensor ($I_1 = \mathrm{tr}\,\boldsymbol{\sigma}$) and the $y$-axes variable $\sqrt{J_2}$ is the square root of the second "mechanics" invariant of stress ($J_2 = \boldsymbol{\sigma}'\!:\!\boldsymbol{\sigma}'$) . . . . . 17

2.2 Dilatant plastic flow occurs in materials in which the shear strength increases with confining pressure. The simplest constitutive models to capture this type of behavior are the linear and nonlinear Drucker-Prager models shown. . . . . 22

2.3 Kayenta continuous yield surface. (a) three-dimensional view in principal stress space with the high pressure cap shown as a wire frame, (b) the meridional side view with the cap shown on the more compressive right-hand side of the plot using cylindrical coordinates in which z points along the compressive [111] direction, and (c) the octahedral view, which corresponds to looking down the hydrostat (onto planes perpendicular to the [111] direction); an option is available for a pressure-varying octahedral profile. . . . . 23

2.4 Demonstration of some effects of elastic-plastic coupling on prediction of pressure and volumetric strain for porous sandstone. Clearly, neglecting $\boldsymbol{z}$ leads to a large increase in predicted pressure and unrealistic predictions for total volumetric strain. . . . . 24

2.5 Softening, the progressive loss of strength, initiates at a predefined criterion . 25

3.1 Return to the spall cut plane used for tensile control. . . . . 30

3.2 Prescribed deformation path for the described example problem. . . . . 31

3.3 Dilatant plastic flow occurs in materials in which the shear strength increases with confining pressure. The simplest constitutive models to capture this type of behavior are the linear and nonlinear Drucker-Prager models shown. . . . . 32

4.1 Screen capture of the Payette GUI . . . . . 36

4.2 Screen capture of the Payette visualization tool . . . . . 37

4.3 Screen capture of an optimization simulation in which the elastic bulk and shear moduli (opt_k and opt_g in the legend) were optimizd to data in the file exmpls.gold. The final simulation is nearly indistiguishable from the gold results. . . . . 39

# List of Tables

# Chapter 1

# Introduction

When simulating events involving extremes in pressure as a consequence of blast, penetration, and shock loadings, among others, it is necessary to describe the hydrostatic material response by an equation of state. When material strength cannot be neglected, an additional constitutive model must be incorporated to describe the material's deviatoric response as part of the stress update algorithm. For elastic-perfectly-plastic materials, the deviatoric response is separable from the hydrostatic response and its incorporation with an arbitrary equation of state in a total stress update is straightforward. However, for materials in which the hydrostatic and deviatoric responses are not separable, combining an equation of state and strengh models becomes problematic. The hydrostatic response is not solely a function of the pressure computed by the equation of state. Neglecting the hydrostatic/deviatoric coupling leads to inconsistent material states and can, ultimately, lead to unstable finite element simulations.

The focus of this Early Career Lab Directed Research and Development (ECLDRD) project (referred to simply as the project in the body of this report), focused on the development of constitutive softening routines in the Kayenta material model [2, 7] and integration of the Kayenta in the Alegra [14] finite element code. The target application was predicting depth of penetration in hardened ceramic armor. A summary of key accomplishments. While the target application was narrow in focus, this project made wide ranging impacts in several areas of strategic interest to SNL:

**Sierra SM Integration** Early efforts focused on integrating Kayenta in to the Sierra SM suite of finite element codes. Integration included coupling the Kayenta softening schemes with Sierra's multi-level control failure framework, creation of new elastic moduli fitting functions, and continued development of Kayenta's orthotropic jointing capabilities.

Payette **development** Payette is a material model development toolkit that was developed as an environment for material model development. Payette allows for rapid development and testing of new constitutive features. Additionally, Payette provides analysts tools for determining parameter sensitivity and optimization.

**Kayenta model development** The core of the project centered around development of thermodynamically consistent incorporation of high pressure equation of state in Kayenta and constitutive descriptions of material damage and softening. The existing time to

failure softening model was supplemented by total and plastic strain to failure descriptions. A novel spall failure criterion was developed and implemented.

ALEGRA **Integration** Equation of state and damage routines in Kayenta were integrated in to the ALEGRA finite element code.

The research activities in this project have already resulted production ready technologies that are making impacts in other projects internal and external to SNL. The work is currently being leveraged in several projects at SNL [11, 3] and researchers at the Army Research Labs are currently using the work in their investigations.

This report describes efforts during the latter half of fiscal year 2012 and beginning of fiscal year 2013. Chapter 4 describes the PAYETTE material model driver and presents the advantages of developing constitutive models in a stand alone tool. Chapters 2 and 3 describe the Kayenta material model, developments in damage routines, and coupling with a high pressure equation of state and ALEGRA. Finally, concluding remarks are made in 5.

# Chapter 2

# The Kayenta Material Model

Kayenta, an outgrowth of the Sandia GeoModel [2], is a general three invariant phenomenological plasticity model developed for use with geological and rock-like engineering materials. Like most classical plasticity models, Kayenta presumes that a boundary between elastically obtainable stress states and stress states unobtainable through inviscid processes exists and is called the *yield surface*. Mathematically, the yield surface is expressed in terms of a stress dependent *yield function* $f(\boldsymbol{\sigma})$. The *yield criterion* is the statement that $f(\boldsymbol{\sigma}) \leq 0 \ \forall \ \boldsymbol{\sigma}$. We say that a material has yielded if for a *trial elastic stress* $\boldsymbol{\sigma}^{\text{trial}}$, the yield criterion is violated, or $f\left(\boldsymbol{\sigma}^{\text{trial}}\right) > 0$. In this case, the material is said to "flow" plastically. The goal of the plasticity problem then becomes finding the portion of the strain rate attributible to plastic deformation such that the yield criterion is satisfied and the solution advanced. In this chapter, an overview of Kayenta is presented. For further details, consult [2].

## 2.1 Elasticity

Kayenta supports both linear and nonlinear elasticity, and presumes that the material *and* its elastic stiffness are isotropic[1]and obey Hooke's law

$$\dot{\boldsymbol{\sigma}} = \mathbb{C}\!:\!\dot{\boldsymbol{\varepsilon}}^e = \kappa \dot{\varepsilon}_v^e \boldsymbol{\delta} + 2\mu \dot{\boldsymbol{\gamma}}^e \tag{2.1}$$

where $\dot{\boldsymbol{\varepsilon}}^e$ is the rate of elastic strain (with $\dot{\varepsilon}_v^e$ its volumtric part and $\dot{\boldsymbol{\gamma}}^e$ its deviatoric part), $\boldsymbol{\delta}$ is the second-order identity tensor, and $\kappa$ and $\mu$ are the nonlinear elastic bulk and shear moduli functions, given by

$$\kappa = b_0 + b_1 \mathrm{e}^{-b_2/|I_1|} - b_3 \mathrm{e}^{-b_4/|\varepsilon_v^p|}, \qquad \mu = g_0 \left( \frac{1 - g_1 \mathrm{e}^{-g_2\sqrt{J_2}}}{1 - g_1} \right) - g_3 \mathrm{e}^{-g_4/\gamma_{eq}^p} \tag{2.2}$$

and the $b_i$ and $g_i$, $\varepsilon_v^p$, and $\gamma_{eq}^p$ are model fitting parameters, platic volume strain, and scalar plastic shear strain, respectively.

Kayenta presumes that the rate of strain $\dot{\boldsymbol{\varepsilon}}$ is the sum of elastic and plastic components[2], $\dot{\boldsymbol{\varepsilon}} = \dot{\boldsymbol{\varepsilon}}^e + \dot{\boldsymbol{\varepsilon}}^p$, so that the stress/strain relationship in Equation (2.1) can instead be expressed

$$\dot{\boldsymbol{\sigma}} = \kappa \left( \dot{\varepsilon}_v - \dot{\varepsilon}_v^p \right) \boldsymbol{\delta} + 2\mu \left( \dot{\boldsymbol{\gamma}} - \dot{\boldsymbol{\gamma}}^p \right), \tag{2.3}$$

[1]Material isotropy does not necessarily imply isotropy of the elastic stiffness [6, 5]

[2]Here, and throughout the report, plasticity refers to any inelastic process

where $\dot{\varepsilon}_v$, $\dot{\varepsilon}_v^p$, $\dot{\boldsymbol{\gamma}}$, $\dot{\boldsymbol{\gamma}}^p$ are the volumetric and deviatoric parts of the total and plastic strain rates, respectively.

The plasticity problem begins by tentatively assuming that the entire stress increment is elastic ($\dot{\boldsymbol{\varepsilon}}^p = \mathbf{0}$), thus producing a "trial" stress $\boldsymbol{\sigma}^{\text{trial}}$. If $f\left(\boldsymbol{\sigma}^{\text{trial}}\right) \leq 0$, the trial stress becomes the updated stress and the solution is complete. If, on the other hand, $f\left(\boldsymbol{\sigma}^{\text{trial}}\right) > 0$, plastic flow occurs and the equations of elasticity must be suplemented by the equations of plasticity.

## 2.2 Plastic Flow

Representing the rate of plastic strain as the product of its magnitude $\dot{\lambda}$ and (unit) direction $\boldsymbol{m}$, the rate of stress in Equation (2.3) becomes

$$\dot{\boldsymbol{\sigma}} = \left(\kappa\dot{\varepsilon}_v - \frac{1}{3}\dot{\lambda}\,\mathrm{tr}\,\boldsymbol{p}\right)\boldsymbol{\delta} + 2\mu\dot{\boldsymbol{\gamma}} - \dot{\lambda}\boldsymbol{p}', \tag{2.4}$$

where $\boldsymbol{p} = \mathbb{C}\!:\!\boldsymbol{m}$ is the plastic return direction and $\boldsymbol{p}' = \dot{\lambda}\left(\boldsymbol{p} - 1/3\,\mathrm{tr}\,\boldsymbol{p}\boldsymbol{\delta}\right)$ is its deviatoric part[3]. In the literature, one encounters several definitions of the plastic flow direction $\boldsymbol{m}$, given by

$$\boldsymbol{m} = \frac{\partial\phi\left(\boldsymbol{\sigma}\right)}{\partial\boldsymbol{\sigma}} \Big/ \left\|\frac{\partial\phi\left(\boldsymbol{\sigma}\right)}{\partial\boldsymbol{\sigma}}\right\| \tag{2.5}$$

where $\phi$ is a "flow potential". If $\phi = f$, the plastic flow is said to be associative, otherwise the flow is non-associative. It should be noted, that non-associative plastic is known to violate thermodynamics [15, 12], though it is still commonly adopted. Kayenta supports both associative and non-associative plastic flow, with this caveat.

### 2.2.1 Isochoric Plastic Flow

Isochoric plastic flow is plastic flow occurs in materials that exhibit plastic incompressibility during plastic loading. In these materials, the strength is independent of the confining pressure, consequently, the plastic flow and return direction are purely deviatoric, as shown in Figure 2.1. In this case $\mathrm{tr}\,\boldsymbol{p} = 0$ and the stress/strain relationship in Equation (2.4) reduces to

$$\dot{\boldsymbol{\sigma}} = \kappa\dot{\varepsilon}_v\boldsymbol{\delta} + 2\mu\left(\dot{\boldsymbol{\gamma}} - \dot{\lambda}\boldsymbol{m}'\right). \tag{2.6}$$

In other words, the deviatoric response is fully decoupled from the hydrostatic response. The Von Mises yield criterion is an example of a yield criterion that emits isochoric plastic flow and is appropriate for materials such as most metals in which the assumption of plastic incompressibility is acceptable.

[3]Throughout, the $'$ indicates the deviatoric part of the argument.

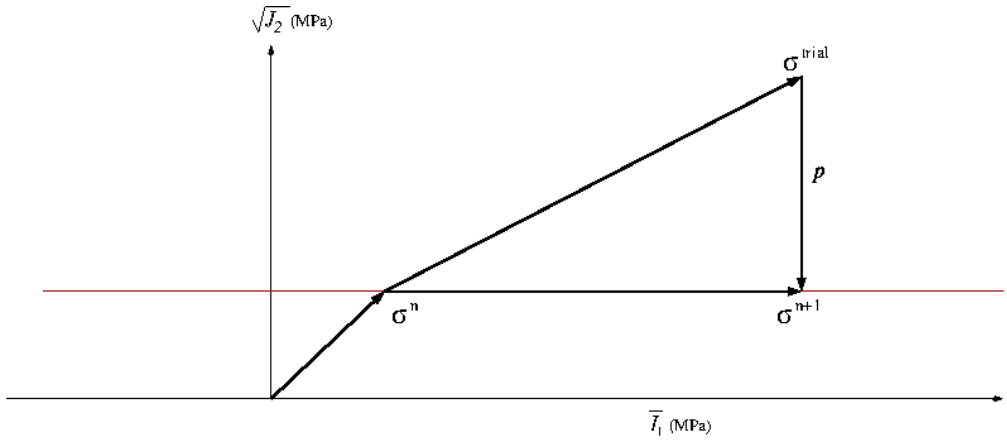


**Figure 2.1.** Deviatoric return direction results in isochoric plastic flow for the Von Mises yield criterion. The $x$-axes variable $\bar{I}_1$ is the *negative* of the first invariant of the stress tensor ($I_1 = \operatorname{tr} \boldsymbol{\sigma}$) and the $y$-axes variable $\sqrt{J_2}$ is the square root of the second "mechanics" invariant of stress ($J_2 = \boldsymbol{\sigma}' \!:\! \boldsymbol{\sigma}'$)

### 2.2.2 Dilatant Plastic Flow

Dilatant plastic flow occurs in materials that exhibit plastic compressibility during plastic loading. In these materials, the strength is dependent on the confining pressure and the plastic flow has a hydrostatic component, in addition to the deviatoric component described above and as shown in Figure (2.2). In this case, the stress/strain relationship in Equation (2.4) cannot be decoupled in to independent hydrostatic and deviatoric components.

The linear/nonlinear Drucker-Prager yield criterion are examples of yield criteria that emit dilatant plastic flow and are appropriate for materials in which strength increases with confining pressure, such as geologic and engineered geologic-type materials. For materials that also exhibit an upper limit in the amount of supportable hydrostatic pressure, the yield function is enhanced with the addition of a "cap" on the upper limit of hydrostatic pressure.

## 2.3 The Kayenta Limit Surface

Kayenta adopts a continous nonlinear yield surface that combines features of a nonlinear Drucker-Prager surface with a cap in a phenomenological manner. The yield function is given by

$$f\left(\boldsymbol{\sigma}\right) = \Gamma^2\left(\Theta\right) J_2 - f_f^2\left(I_1\right) f_c^2\left(I_1, \kappa\right) J_2 \tag{2.7}$$

where $I_1$, $J_2$, and $\Theta$ are three independent invariants of the stress tensor $\boldsymbol{\sigma}$ and its deviator $\boldsymbol{s}$:

$$I_1 = \operatorname{tr} \boldsymbol{\sigma}, \quad J_2 = \frac{1}{2} \operatorname{tr} \boldsymbol{s}^2, \quad J_3 = \frac{1}{3} \operatorname{tr} \boldsymbol{s}^3, \quad \sin 3\Theta = -\frac{J_3}{2} \left( \frac{3}{J_2} \right)^{3/2} \tag{2.8}$$

$f_f$ is a nonlinear Drucker-Prager yield function that governs material behavior in shear dominated loadings, given by

$$f_f = a_1 - a_3 \mathrm{e}^{-a_2 I_1} - a_4 I_1 \tag{2.9}$$

where the $a_i$ are fitting parameters.

$f_c$ is a nonlinear Pelessone function "cap" function that governs the behavior of porous media during hydrostatically dominated loadings, given by

$$f_c = \sqrt{1 - \left( \frac{I_1 - \kappa}{X - \kappa} \right)^2} \tag{2.10}$$

where $\kappa$ and $X$ are variables representing the evolution of pores in the material.

Finally, the multiplier function $\Gamma$ on $J_2$ is a function of $\Theta$ whose form varies depending on user inputs and allows Kayenta to match observations that quasi-brittle materials are generally weaker in triaxial extension than triaxial compression.

Depending on the choice of model parameters, Kayenta is capable of producing, among others, any of the following features

- Linear and nonlinear thermoelasticity.
- Von Mises and Tresca thermoplasticity.
- Linear and nonlinear, associative and nonassociative Drucker-Prager, Mohr-Coulomb, and Willam-Warnke plasticity.
- Rate-independent or strain-rate sensitive yield.
- Damage through the loss of stiffness and strength.
- Evolution of porosity.
- Pressure- and shear-dependent compaction (similar to $p$-$\alpha$ models during hydrostatic loading, but generalized to include shear effects in general loading).

Kayenta has been used in applications ranging from quasistatic loading of sandstone caprock during $CO_2$ sequestration, ductile fracture of metals, to brittle fracture of ceramic armor systems.

## 2.4 Elastic-Plastic Coupling

The cap model is utilized to allow for plastic reduction of volume due to permanent reduction in pore space. Elastic moduli are also allowed to vary with plastic strain by including dependence on the plastic strain in (2.2), this is the origin of the so called elastic-plastic coupling. While elastic-plastic coupling is observed in porous materials, such as rock and concrete, its inclusion in the constitutive response requires more than merely altering the forms of the elastic moduli. Indeed, consistent inclusion of elastic-plastic coupling requires altering the equations of plasticity as described in [1, 8]. Here we demonstrate some dramatic results of implementing elastic-plastic coupling in a consistent manner.

Let the stress be linear in elastic strain

$$\boldsymbol{\sigma} = \boldsymbol{\sigma}\left(\boldsymbol{\varepsilon}^e, \hat{\kappa}\right) \tag{2.11}$$

where $\hat{\kappa}$ the history dependent secant bulk modulus. Then

$$\dot{\boldsymbol{\sigma}} = \mathbb{C}\!:\!\dot{\boldsymbol{\varepsilon}}^e + \frac{\partial \boldsymbol{\sigma}}{\partial \hat{\kappa}}\dot{\hat{\kappa}} \tag{2.12}$$

The history dependent bulk modulus is presumed to evolve proportionally with the plastic strain:

$$\dot{\hat{\kappa}} = h_{\hat{\kappa}}\dot{\lambda} \tag{2.13}$$

giving for $\dot{\boldsymbol{\sigma}}$ in (2.12)

$$\begin{aligned} \dot{\boldsymbol{\sigma}} &= \mathbb{C}\!:\!\dot{\boldsymbol{\varepsilon}}^e + \frac{\partial \boldsymbol{\sigma}}{\partial \hat{\kappa}} h_{\hat{\kappa}}\dot{\lambda} \\ &= \mathbb{C}\!:\!\dot{\boldsymbol{\varepsilon}}^e - \boldsymbol{z}\dot{\lambda} \end{aligned} \tag{2.14}$$

where $h_{\hat{\kappa}}$ is the secant bulk modulus "ISV modulus". The specific form for $h_{\hat{\kappa}}$ will be derived in the following section. With the addition of the "$z$" tensor $\boldsymbol{z}$, in (2.14), (2.3) becomes

$$\dot{\boldsymbol{\sigma}} = \mathbb{C}\!:\!\dot{\boldsymbol{\varepsilon}} - \dot{\lambda}\boldsymbol{p}, \qquad \boldsymbol{p} = \mathbb{C}\!:\!\boldsymbol{m} - \boldsymbol{z} \tag{2.15}$$

### 2.4.1 Form of the $z$ Tensor

The form of $\boldsymbol{z}$ depends on the plastic strain dependence of the elastic moduli. Consider the standard secant relationship relating the elastic strain to the stress

$$\boldsymbol{\varepsilon}^e = \hat{\mathbb{S}}\!:\!\boldsymbol{\sigma} \tag{2.16}$$

where $\hat{\mathbb{S}}$ is the stress and plastic strain dependent secant compliance. Supposing that the compliance depends only on the plastic volumetric strain $\varepsilon_v^p$, the rate of elastic strain is then given by

$$\dot{\boldsymbol{\varepsilon}}^e = \left(\frac{\partial \hat{\mathbb{S}}}{\partial \boldsymbol{\sigma}}\!:\!\dot{\boldsymbol{\sigma}} + \frac{\partial \hat{\mathbb{S}}}{\partial \varepsilon_v^p}\dot{\varepsilon}_v^p\right)\!:\!\boldsymbol{\sigma} + \hat{\mathbb{S}}\!:\!\dot{\boldsymbol{\sigma}} \tag{2.17}$$

If $\hat{\kappa} = \hat{\kappa}\left(p, \varepsilon_v^p\right)$, then it can be shown that

$$\boldsymbol{z} = -\frac{p\kappa}{\hat{\kappa}^2}\frac{\partial\hat{\kappa}}{\partial\varepsilon_v^p}\frac{\partial\phi}{\partial I_1}\boldsymbol{\delta} \tag{2.18}$$

Similar arguments lead to a deviatoric component to $\boldsymbol{z}$ due to the dependence of the shear modulus on plastic strain.

## 2.5 Magnitude of the Plastic Strain Rate: The Consistency Condition

Combining the preceding equations, the rate of stress in the plasticity problem is

$$\dot{\boldsymbol{\sigma}} = \mathbb{C}\!:\!\dot{\boldsymbol{\varepsilon}} - \boldsymbol{p}\dot{\lambda}, \qquad \boldsymbol{p} = \mathbb{C}\!:\!\boldsymbol{m} + \boldsymbol{z} \tag{2.19}$$

The only unknown in equation (2.19) is $\dot{\lambda}$ and is found by demanding that during and after a plastic loading step the stress state remain on the yield surface, which leads to the consistency condition that

$$\dot{f} = \frac{\partial f}{\partial\boldsymbol{\sigma}}\!:\!\left(\mathbb{C}\!:\!\dot{\boldsymbol{\varepsilon}} - \boldsymbol{p}\dot{\lambda}\right) + \frac{\partial f}{\partial\kappa}h_\kappa\dot{\lambda} = 0 \tag{2.20}$$

which is solved for $\dot{\lambda}$ in an iterative manner.

### 2.5.1 Some Effects of Elastic-Plastic Coupling

The effects of $\boldsymbol{z}$ on the model response was investigated and some results shown in Figure 2.4. In Figure 2.4, normalized pressure is plotted against total volumetric strain for hydrostatic compression of porous sandstone. The results clearly demonstrate the dramatic effect of including, or not, elastic-plastic coupling in a consistent manner.

In these simulations, neglecting $\boldsymbol{z}$ results in a 52% increase in predicted pressure and a 120% decrease in predicted volume strain. A more complete presentation of the effects of elastic-plastic coupling can be found in [8].

## 2.6 Softening

Kayenta supports the progressive loss of strength by allowing the limit surface to reduce in size due to accumulated damage, as depicted in Figure 2.5. As described in [2], the progressive loss of strength is governed by a time to failure model predicated on the observation

that cracks propogate at a fixed speed. Significant time and effort was spent developing alternative softening models allowing for total and plastic strain based damage accumulation. Softening model development was carried out in conjunction with M. Scot Swan at the University of Utah and is described in detail in [16].

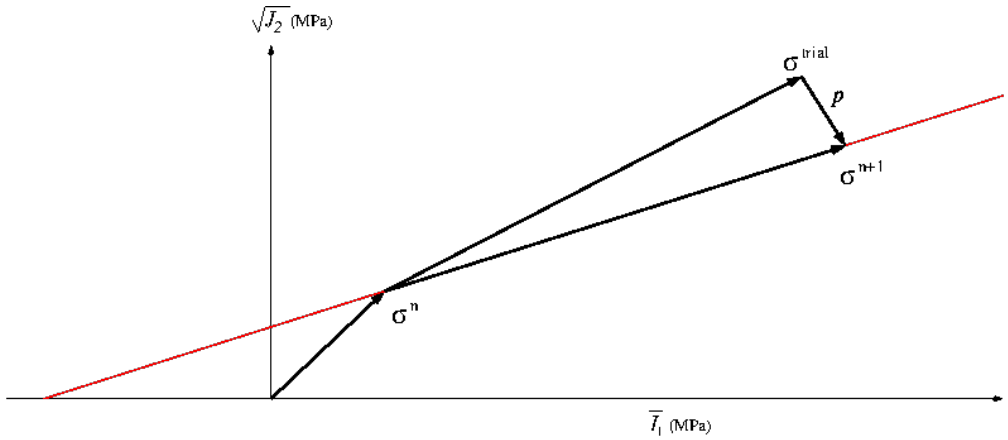


**(a)** Meridional view of the linear Drucker-Prager yield surface

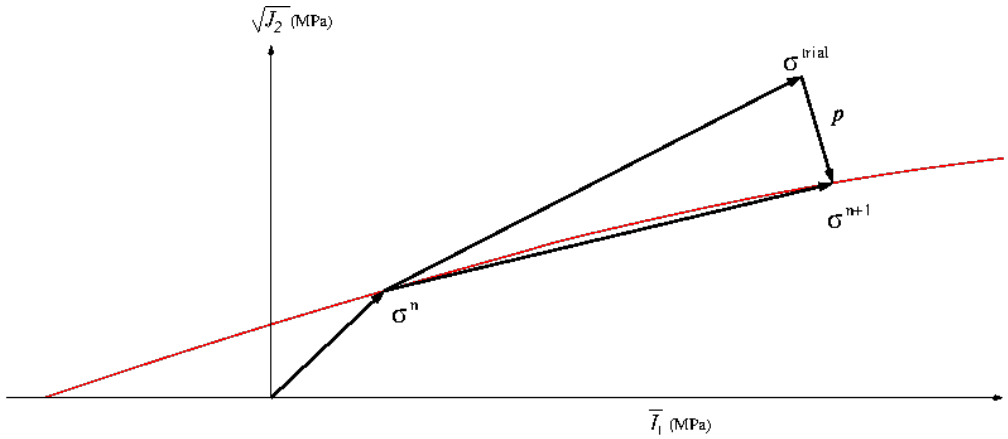


**(b)** Meridional view of the nonlinear Drucker-Prager yield surface

**Figure 2.2.** Dilatant plastic flow occurs in materials in which the shear strength increases with confining pressure. The simplest constitutive models to capture this type of behavior are the linear and nonlinear Drucker-Prager models shown.

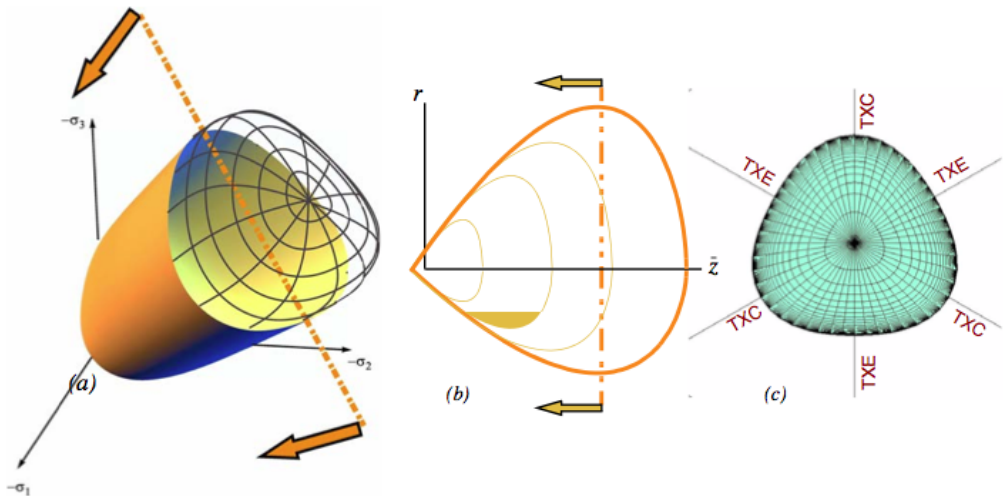


**Figure 2.3.** Kayenta continuous yield surface. (a) three-dimensional view in principal stress space with the high pressure cap shown as a wire frame, (b) the meridional side view with the cap shown on the more compressive right-hand side of the plot using cylindrical coordinates in which z points along the compressive [111] direction, and (c) the octahedral view, which corresponds to looking down the hydrostat (onto planes perpendicular to the [111] direction); an option is available for a pressure-varying octahedral profile.

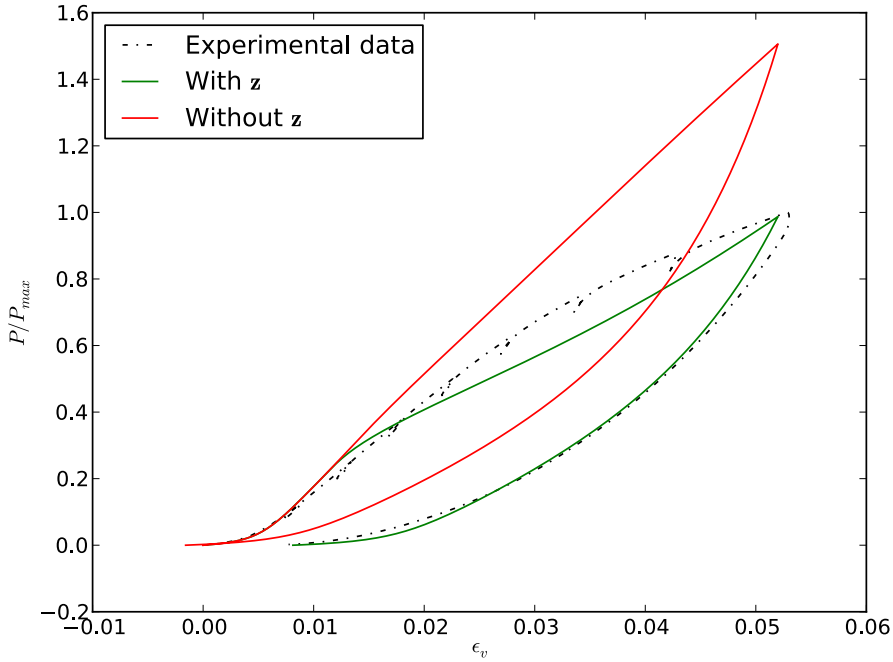


**Figure 2.4.** Demonstration of some effects of elastic-plastic coupling on prediction of pressure and volumetric strain for porous sandstone. Clearly, neglecting $\boldsymbol{z}$ leads to a large increase in predicted pressure and unrealistic predictions for total volumetric strain.

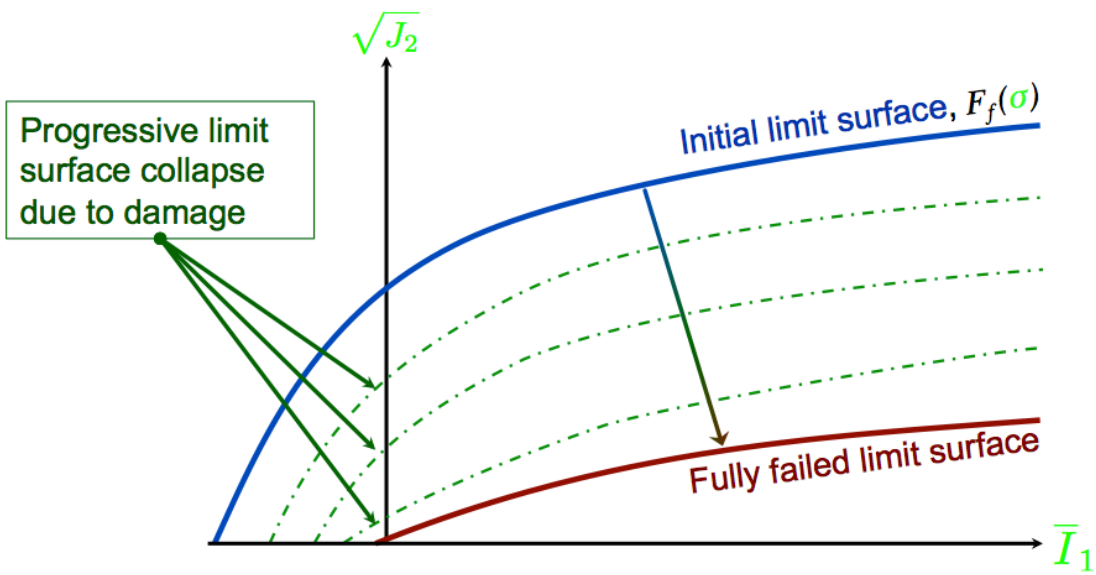


**Figure 2.5.** Softening, the progressive loss of strength, initiates at a predefined criterion

# Chapter 3

# Response of Quasi-brittle Materials in Shock-Hydrocode Simulations

The contents of this chapter are a summary of a presnetation and paper at the ARL Research in Ballistic Protection Technologies Workshop [10]

## 3.1 Coupling the Response of Kayenta with an Equation of State

As explained in 2.2.1, if a material exhibits incompressible plastic flow, the stress/strain relationship of Equation (2.4) is separable in to hydrostatic and deviatoric components. In this case, incorporating an equation of state response with the deviatoric response involves replacing the hydrostatic component $\kappa\dot{\varepsilon}_v\boldsymbol{\delta}$ of Equation (3.1) with the pressure response $P_{eos}$ from an arbitrary equation of state

$$\dot{\boldsymbol{\sigma}} = -\dot{P}_{eos}\boldsymbol{\delta} + 2\mu\left(\dot{\boldsymbol{\gamma}} - \dot{\lambda}\boldsymbol{m}'\right). \tag{3.1}$$

For plastically compressible materials, dilatant plastic flow prohibits the decoupling of the hydrostatic and deviatoric responses, as in Equation (3.1). Instead, the material response is computed from the more general expression of Equation (2.4)

$$\dot{\boldsymbol{\sigma}} = -\dot{P}\boldsymbol{\delta} + 2\mu\left(\dot{\boldsymbol{\gamma}} - \dot{\lambda}\boldsymbol{m}'\right). \tag{3.2}$$

where we have substituted $\dot{P} = \kappa\dot{\varepsilon}_v - 1/3\dot{\lambda}\,\mathrm{tr}\,\boldsymbol{p}$. Comparing Equations (3.1) and (3.2), if the hydrostatic/deviatoric coupling is neglected, discrepancies are seen to arise as $P_{eos}$ deviates from $P$. Such an inconsistency leads to further inconsistencies in other material variables computed from the equation of state including the soundspeed, density, and ultimately, the stable timestep. It was found that in Alegra [14] these iconsistencies ultimately manifest themselves in simulations that end prematurely due to unresolvably bad material states.

The approach developed in Alegra to resolve the above inconsistencies is an iterative approach similar to the Alegra multi-material treatment [13], whereby the bulk modulus

is given by

$$\kappa = \rho_\star c_{\mathrm{s}}^2(u, \rho_\star), \tag{3.3}$$

where $c_{\mathrm{s}}$ is the energy and density dependent sound speed returned by the equation of state, and $\rho_\star$ is the "solid density" of the material. Using $\kappa$, the pressure is updated by

$$\dot{P} = \kappa \dot{\varepsilon}_v - \frac{1}{3}\dot{\lambda}\,\mathrm{tr}\,\boldsymbol{p}, \tag{3.4}$$

and the solid density updated iteratively by

$$\rho_\star^n = \rho_\star^{n-1} + \frac{P - P_{eos}^{n-1}}{dP/d\rho_\star}. \tag{3.5}$$

Convergence is achieved when $P = P_{eos}$. In this way, the discrepancy between the mean response of the constitutive model and the pressure response of the equation of state is eliminated. The solid density $\rho_\star$ is interpreted as the density of the intact material absent the presence of void.

As an example of an inconsistency that can develop between the constitutive model and host finite element code, consider a case of pure shear of a single element of Kayenta material. During pure shear, the deformation is isochoric and pressure changes computed by the equation of state are small in comparison to changes in the mean stress computed from the constitutive model.

## 3.2 Tensile Control in Shock-Hydrocode Simulations

Control of excessive tension for non-gaseous materials becomes necessary when the deformation of the material indicates expansion to an unphysical density. Generally, equation of state models will break down under such conditions unless specific action is taken to detect and mitigate the excessive tension. The physical observation for material under these conditions is fracture for solids and cavitation for liquids.

In the Alegra code, the method for controlling excessive tension involves limiting the pressure of the material to a relaxed value less tensile than would be indicated by the expansion of the element. This results in an increased density and, consequently, a decrease in material volume fraction to satisfy mass conservation. The difference in volume is taken up by an increase in the void volume fraction.

The density associated with the relaxed pressure is obtained using an iterative with pressure computed from the equation of state as a function of density and internal energy, $P_{eos} = P_{eos}(u, \rho)$.

Density iterations are estimated from $dP_{eos}/d\rho$ and evaluated until the pressure computed by the equation of state converges to the relaxed pressure. While other codes may use other approaches to controlling excessive expansion, this "Void Insertion" approach is used by

Alegra. However, this void insertion method implicitly assumes that the pressure is only a function of the equation of state and is equivalent to the mean stress of the material. With the Kayenta material model, this assumption cannot be guaranteed, particularly for dilatant behavior. Thus, the standard tensile control in Alegra cannot be utilized with the Kayenta material model, or any other material in which dilatant plastic flow is allowed. Instead, the following approach has been implemented to allow consistent response between the equation of state model and the tensile response computed in the Kayenta material model.

Returning to the assumption of the additive decomposition of the total strain in to elastic and plastic parts, the plastic strain rate is further subdivided in to parts due to plasticity and void expansion such that the elastic strain rate is now given by

$$\dot{\boldsymbol{\varepsilon}}^e = \dot{\boldsymbol{\varepsilon}} - \dot{\boldsymbol{\varepsilon}}^{\text{void}} - \dot{\boldsymbol{\varepsilon}}^p \tag{3.6}$$

where $\dot{\boldsymbol{\varepsilon}}^p$ is the strain rate due to plasticity and $\dot{\boldsymbol{\varepsilon}}^{\text{void}}$ that due to void expansion. We assume that void expansion is a purely hydrostatic process so that its rate is given by

$$\dot{\boldsymbol{\varepsilon}}^{\text{void}} = \dot{\lambda}^{\text{void}} \hat{\boldsymbol{\delta}} \tag{3.7}$$

where $\hat{\boldsymbol{\delta}}$ is the normalized second order identity tensor and $\dot{\lambda}^{\text{void}}$ the magnitude of the rate of void strain.

The onset of excessive tensile deformation is marked by $P > P_{spall}$ where $P_{spall}$ is a material parameter representing the value of pressure at which spall is observed to occur. Analogous to computing $\dot{\lambda}$ such that the yield criterion is satisfied, $\dot{\lambda}^{\text{void}}$ is computed such that the spall criterion $P \leq P_{spall}$:

$$P^{n+1} = P^n + \dot{P}^n \Delta t = P^n + 3\kappa \operatorname{tr}\left(\dot{\boldsymbol{\varepsilon}} - \dot{\lambda}^{\text{void}} \hat{\boldsymbol{\delta}} - \dot{\lambda} \boldsymbol{m}\right) \Delta t \geq P_{spall},$$

thus, we compute $\dot{\lambda}^{\text{void}}$ by

$$\dot{\lambda}^{\text{void}} = \begin{cases} 0 & \text{if } P^{n+1} \geq P_{spall} \\ \frac{1}{\sqrt{3}} \left( \dot{\varepsilon}_v - \dot{\lambda} \operatorname{tr} \boldsymbol{m} - \frac{P_{spall} - P^n}{3\kappa \Delta t} \right) & \text{if } P^{n+1} < P_{spall} \end{cases} \tag{3.8}$$

Kayenta then returns both the updated stress $\boldsymbol{\sigma}$ *and* the magnitude of the void strain increment $\dot{\lambda}^{\text{void}}$ to Alegra and the material volume fraction adjusted such that mass is conserved.

Figure 3.1 depicts graphically the return of the trial stress to the yield surface and then to spall-cut plane.

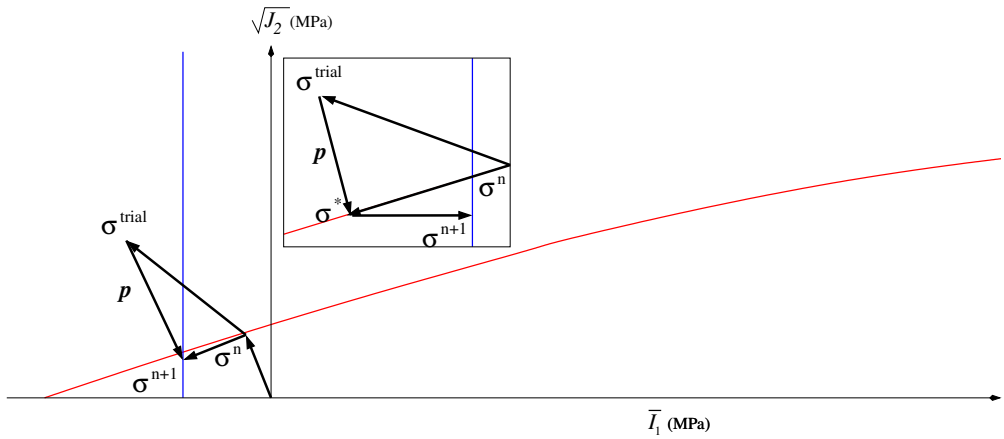


**Figure 3.1.** Return to the spall cut plane used for tensile control.

## 3.3 Comparison of Density with/without Tensile Control

The improved treatment of tensile states is now shown through a simulation designed to demonstrate the density and tensile control outlined in Sections 3.1 and 3.2. In this problem, a single element of Kayenta material is deformed in pure shear, upon reaching a critical value of shear strain the element is then deformed in tension along one of its diagonals, as shown in Figure 3.2. The path through stress space for the problem is also shown.

The density response of the material is shown in Figures 3.3(a) and 3.3(b). In Figure 3.3(a), the pressure and density update in the Kayenta material neglected the hydrostatic/deviatoric coupling. Upon reaching excessive tensile states the density reduces to unphysical levels and the simulation eventually became unstable. There is no distinction between the element density and the solid density. In contrast, the pressure and density updates in Figure 3.3(b) adhered to the methods outlined in Sections 3.1 and 3.2. In this simulation, there is a clear dilineation between the solid density (upper curve) and the element density (lower curve). Upon reaching the tensile limit, void is accumulated in the element, evidenced by the near constant density in the right half of the figure.

## 3.4 Application of Kayenta to Penetration Predictions in Ceramic Armor Systems

A target application of this project was simulating the response of ceramic armor systems to penetration from a high velocity projectile. Extensive mesh sensitivity studies were un-

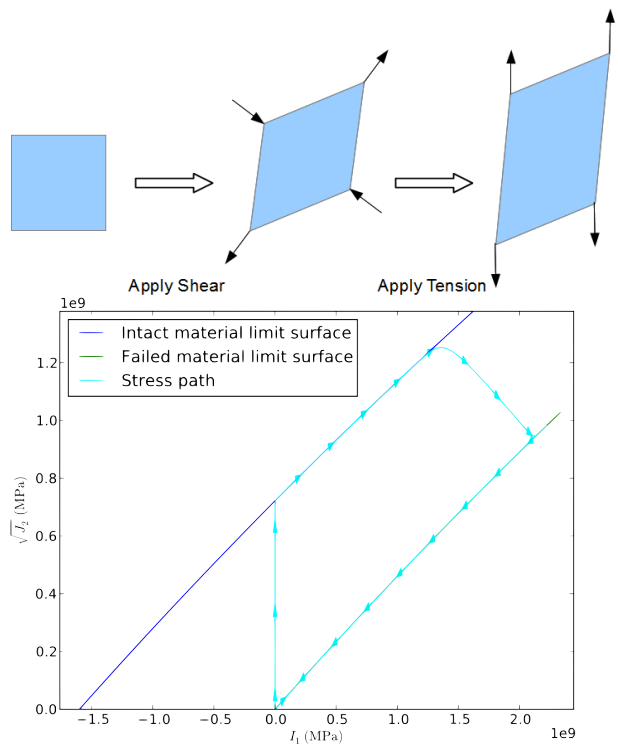


**Figure 3.2.** Prescribed deformation path for the described example problem.

dertaken and documented. In an effort to keep this report as unlimited release, the results of the study are being ommitted, but are available upon request to the first author.

## 3.5 Conclusion

Recent efforts coupling the hydrostatic equation of state response with the deviatoric material response in ALEGRA finite element code were described. The inseperability of the hydrostatic and deviatoric material responses in materials exhibiting dilatant plastic flow were described. Unphysical material densities were shown to occur if the coupling is neglected. A new method of coupling the equation of state response and the deviatoric material was response was shown to resolve unphysical tensile states in a shock-hydrocode simulation, leading to more stable treatment of extreme tensile states common in the simulation of blast and penetration events.

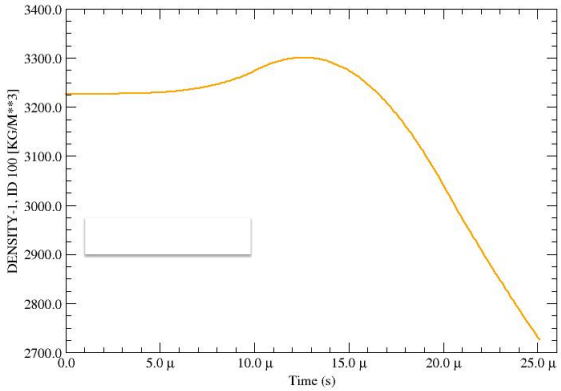


**(a)** Density comparison without the density control described in Sections 3.1 and 3.2

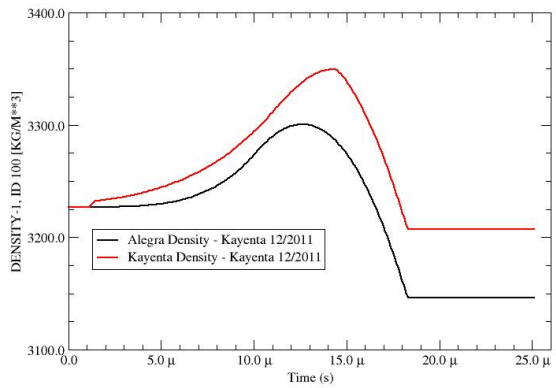


**(b)** Density comparison with the density control described in Sections 3.1 and 3.2

**Figure 3.3.** Dilatant plastic flow occurs in materials in which the shear strength increases with confining pressure. The simplest constitutive models to capture this type of behavior are the linear and nonlinear Drucker-Prager models shown.

# Chapter 4

# Payette, An Object Oriented Material Model Driver

## 4.1 Introduction

A key element of the project was the continued development of algorithms in Kayenta that more realistically model observed material behavior in events that lead to a loss of material strength. To aid in these efforts, Payette [4] was developed for the purpose of constitutive model development and testing. Payette, a suite of tools was originally created by the first author in graduate school, for the purpose of constitutive model development and testing. The suite of tools was further developed as required to complete the project's objectives. Payette has now also been adopted by other organization within SNL who are interested in constitutive model development and understanding. Payette was released as open source software by Sandia Corporation in August 2012. A more detailed report [9] is in preparation, presented here are key features of Payette.

## 4.2 Why a Single Point Material Driver?

Due to their complexity and excessive compile and link times, full-scale finite element codes do not provide an ideal environment for constitutive model development. Additionally, features such as artificial viscosity, hourglass control, and others, can mask the actual material response from the finite element response, making constitutive model development a difficult and more time consuming task than necessary. Being a stand alone material model driver, Payette allows the constitutive model developer to concentrate entirely on the material response during model development by driving the constitutive model directly at a single material point by prescribed forcing functions, thereby eliminating any artifacts of the finite element host code. Verification of constitutive model response and validation against experimental evidence is more easily realized in this stand alone environment. Other advantages of Payette are:

- Payette is a very small, special purpose code. Thus, maintaining and adding new features is very easy.

- Simulations are not affected by irrelevant artifacts such as artificial viscosity or uncertainty in the handling of boundary conditions.
- It is straightforward to produce supplemental output for deep analysis of the results that would otherwise constitute an unnecessary overhead in a finite element code.
- Specific material benchmarks may be developed and automatically run quickly any time the model is changed.
- Specific features of a material model may be exercised easily by the model developer by prescribing strains, strain rates, stresses, stress rates, and deformation gradients as functions of time.
- Rapid development of new model features.

In the author's and other analysts' experience, the use of PAYETTE has led to significant decreases in the time required to develop and implement model features and parameterize constitutive models with experimental data. To follow are descriptions of some key features.

## 4.3 Obtaining and Building PAYETTE

PAYETTE can be obtained by downloading the source code from the central repository [4]. Instructions for building and installing PAYETTE are included with the source code.

## 4.4 PAYETTE: Key Features

### 4.4.1 User Interaction

PAYETTE has two primary modes of interacting with users: formatted plain text input files and a graphical user interface (GUI). PAYETTE returns the result of a simulation in columnar ascii output files.

#### 4.4.1.1 PAYETTE Input File Format

Input files are comprised of several "blocks" of instruction that PAYETTE reads. A block is a group of instructions contained in `begin <block> [block name] ...end <block>` pairs:

```
begin <block> [block name]
        .
```

```
        .
        .
end <block>
```

Input files are case and indentation insensitive and comments are denoted by "#". and require the following blocks: `simulation, material, boundary, legs`

**A Sample Input** The following input describes a kayenta material exercised through a uniaxial strain deformation path

```
begin simulation my_simulation

  begin material
    constitutive model kayenta
    B0 135.e9
    G0 53.e9
    A1 10.e6
  end material

  begin boundary
    begin legs
      tstar = 1.e-6
      using time, strain
      0 0 0 0 0 0 0
      1 1 0 0 0 0 0
    end legs
  end boundary

end simulation
```

**Running** Payette Payette is run through a command line interface as follows

```
$ payette input_file
```

Other options

#### 4.4.1.2 Payette Graphical User Interface

A GUI, shown in Figure 4.1, allows analysts and developers to interact with material models without the need for writing formatted input files. The GUI implements all features available through interacting with Payette through input files.

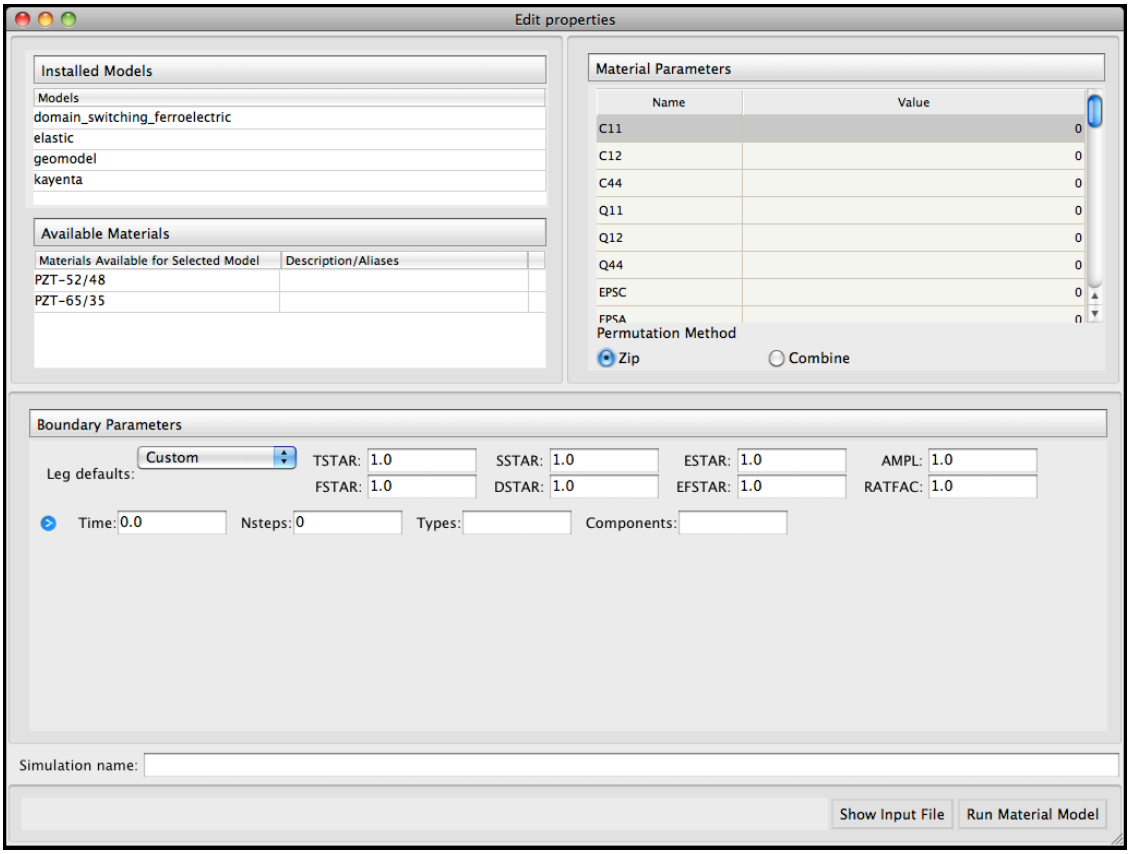


**Figure 4.1.** Screen capture of the PAYETTE GUI

### 4.4.2 Visualization of Constitutive Model Data

In addition to the GUI for running PAYETTE simulations, a visualization toolkit has also been developed for creating 2D plots of model outputs, shown in Figure 4.2.

Being able to implement new model features and then visualize the effects of those features on model results in a rapid fashion has proven invaluable for efficient constitutive model development.

### 4.4.3 Parameter Sensitivity and Optimization

PAYETTE has builtin the ability to assist in understanding the sensitivity of a constitutive model to model parameters by running a batch of simulations using permutated parameters. Additionally, optimized model parameters can be determined by minimizing the difference between simulation outputs and known results by varying model parameters. Instructions for these tasks are given in the `permutation` and `optimization` blocks.

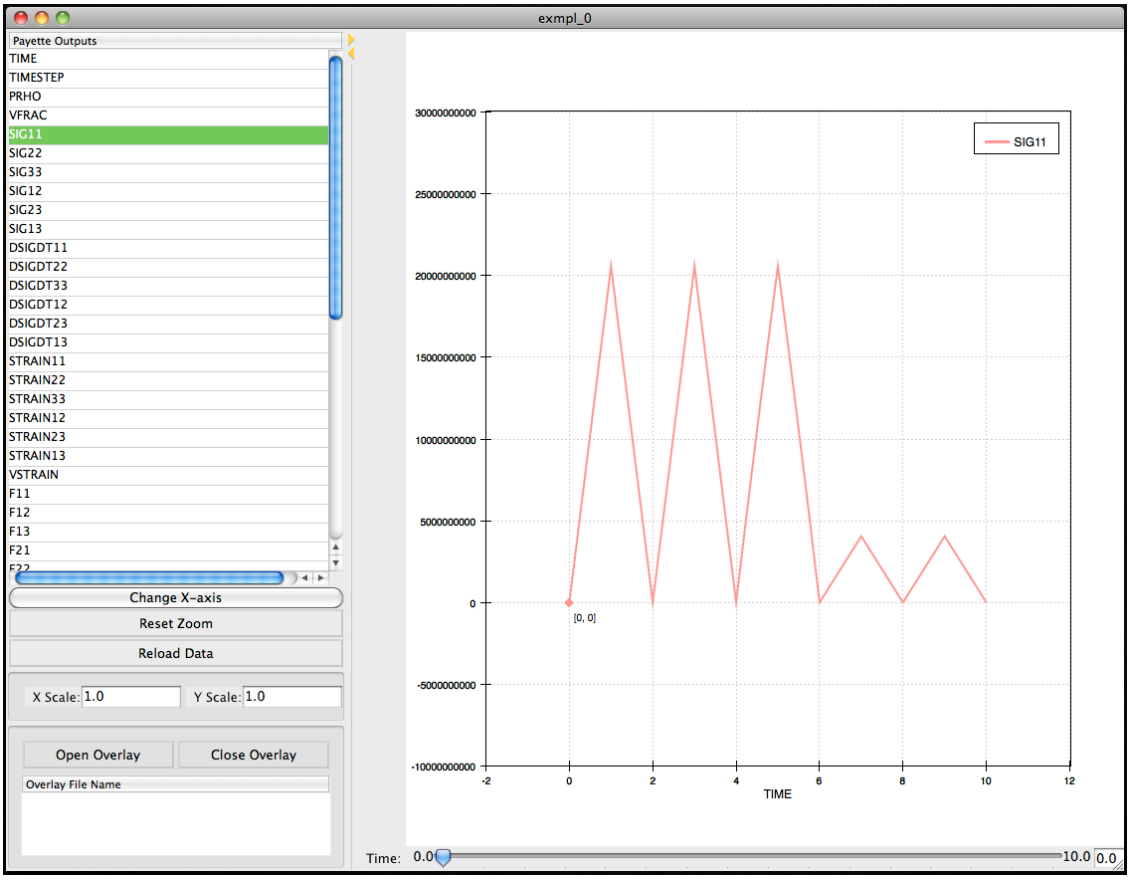


**Figure 4.2.** Screen capture of the PAYETTE visualization tool

#### 4.4.3.1 The `permutation` Block

The `permutation` block is used to run a batch of simulations that are very similar to the base input given. The basic syntax is:

```
begin material
  constitutive model kayenta
  B0 = {PARAM1}
  G0 = {PARAM2}
  ...
end material
begin permutation
  method zip
  permutate PARAM1 VAL1 VAL2 VAL3 ...
  permutate PARAM2 VAL4 VAL5 VAL6 ...
  ...
```

```
end permutation
```

The preceding input spawns simulations where the value of `B0` is replaced with the current value of `PARAM1`, chosen sequentially from `VAL1, VAL2, ....` Similarly for `G0`. Directories containing each individual simulation and its output are stored and mapped so that the results of the permutation job can be visualized and model sensitivity determined.

#### 4.4.3.2 The `optimization` Block

PAYETTE has the ability to assist in the parameterization of material models through an optimization process whereby optimal parameters are found by minimizing errors on selected simulation output. Minimization is performed using SciPy's minimization module. The basic syntax is:

```
begin optimization

  method simplex
  maxiter 25
  tolerance 1.e-4

  optimize K, bounds = (125.e9, 150.e9)
  optimize G, bounds = (45.e9, 57.e9)

  gold file exmpls.gold
  minimize sig11, sig22, sig33 versus time

end optimization
```

In the preceding block, the values of `K` and `G` are optimized by minimizing the composite difference between the simulated `sig11`, `sig22`, and `sig33` and some known to be good `sig11`, `sig22`, and `sig33` in the "gold" file. In Figure 4.3, the results are shown from a selection of the optimization outputs for a simulation in which the elastic bulk and shear moduli were fit by minimizing the difference between normal stresses. `SIG11` from the gold file is shown overlayed on the simulation results, showing the quality of the fit for the optimized parameters.

## 4.5 Conclusion

PAYETTE has proven to be an invaluable tool for the development and study of new constitutive routines. The speed up in development and use of constitutive models is significant

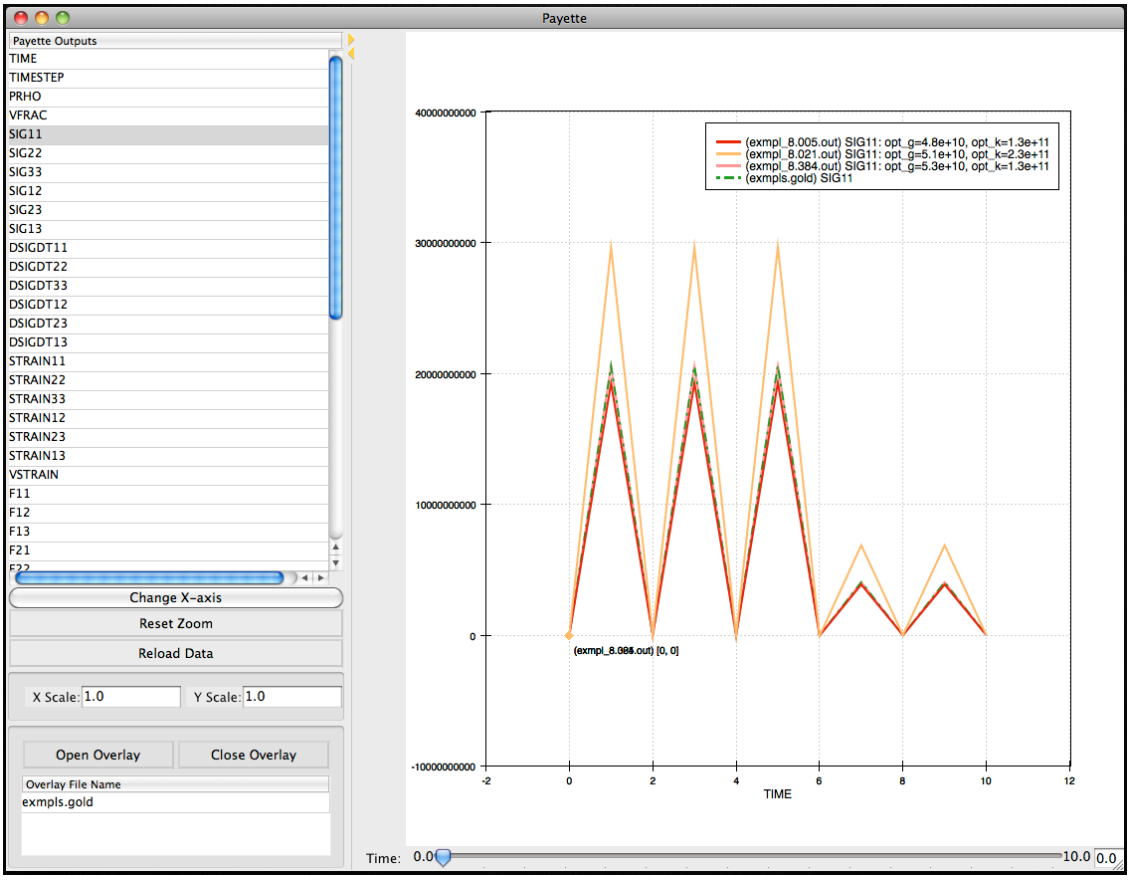


**Figure 4.3.** Screen capture of an optimization simulation in which the elastic bulk and shear moduli (opt_k and opt_g in the legend) were optimizd to data in the file exmpls.gold. The final simulation is nearly indistiguishable from the gold results.

to both model developers and analysts. The influence of PAYETTE is expanding beyond the scope of just this project and has been adopted by a number of analysts and groups at SNL who work in the area of constitutive model development and visualization.

# Chapter 5

# Conclusion

A key focus of this Early Career Lab Directed Research and Development project was the development of constitutive softening routines in the Kayenta material model and itegration of those routines in the ALEGRA finite element code. As a result of this project, several new technologies have been deployed in to production at SNL:

**Kayenta** New algorithms for incorporating in a thermodynamically consistent manner a high pressure equation of state in Kayenta were developed. Improved descriptions of material damage and softening were implemented, including a novel spall failure criterion. New forms of fitting functions for elastic moduli were implemented and orthotropic jointing capabilities enhanced.

**Sierra SM** Kayenta has been deployed in the Sierra SM suite of tools including integration with the multi-level control failure algorithms.

ALEGRA Equation of state and damage routines in Kayenta were fully integrated in release versions of the ALEGRA finite element code.

PAYETTE PAYETTE was developed in conjunction with material modeling efforts as a framework for model development.

# References


[1] Rebecca M. Brannon. Elements of phenomenological plasticity: Geometrical insight, computational algorithms, and topics in shock physics. In Yasuyuki Horie, editor, *Shock Wave Science and Technology Reference Library*, volume 2, pages 225–274. Springer Berlin, 2007.

[2] Rebecca M. Brannon, Arlo F. Fossum, and O. Erik Strack. Kayenta: Theory and User's Guide. Technical Report SAND2009-2282, Sandia National Laboratory, 2009.

[3] T. A. Dewers, P. Newell, S. Broome, J. Heath, and S. Bauer. Elasto-plastic constitutive behavior in three lithofacies of the cambrian mt. simon sandstone, illinois basin, usa. Submitted, 2013.

[4] T. J. Fuller. Payette: An object oriented material model driver. http://payette.github.com/Payette/, 2012.

[5] T. J. Fuller and Rebecca M. Brannon. On the thermodynamic requirement that isotropic materials have an anisotropic stiffness. *Int J Eng Sci*, 49:311–321, 2011.

[6] T. J. Fuller and Rebecca M. Brannon. On the effects of deformation-induced anisotropy on classical elastic-plastic materials. *Int J Num Ana Meth Geo*, Submitted July, 2010.

[7] T. J. Fuller, Rebecca M. Brannon, O. Erik Strack, and J.E. Bishop. Initial inclusion of thermodynamic considerations in Kayenta. Technical Report SAND2010-4687, Sandia National Laboratory, 2010.

[8] T. J. Fuller and Tom Dewers. Some effects of elastic plastic coupling on the fitting of experimental data. In preparation, 2013.

[9] T. J. Fuller and M. Scot Swan. Payette: Theory and user's guide. In preparation, 2013.

[10] T. J. Fuller, M. K. Wong, O. Erik Strack, and M. Scot Swan. Coupling the failure response of brittle materials with eulerian hydro codes in the simulation of high velocity impact. In *ARL Research in Ballistic Protection Technologies Workshop*. Army Research Labs, 2012.

[11] M. J. Martinez, J. E. Newell, P. Bishop, and D. Z. Turner. Coupled multiphase flow and geomechanics model for analysis of joint reactivation during co2 sequestration operations. Accepted, 2013.

[12] T.A. Pucik. A case study of instability and nonuniqueness induced by nonassociated plastic flow. ., 2000.

[13] W.J. Rider, E. Love, M.K. Wong, O.E. Strack, S.V. Petney, and D.A. Labreche. Adaptive methods for multi-material ale hydrodynamics. *Int J Numer Meth Fluids*, 65:1325–1337, 2011.

[14] A.C. Robinson and et al. ALEGRA user manual, version 5.0. Technical Report SAND2010-4796, Sandia National Laboratories, August 2010.

[15] S. Sandler and D. Rubin. The consequences of non-associated plasticity in dynamic problems. In C.D. Desai, editor, *Constitutive Laws for Engineering Materials*, pages 345–352. Elsevier Science Publ. Co., 1987.

[16] M. Scot Swan. *Incorporation of a general strain-to-failure fracture criterion into a stress-based plasticity model through a time-to-failure softening mechanism*. PhD thesis, University of Utah, 2011.

DISTRIBUTION:

| | | |
|---|---|---|
| 1 | MS 0840 | C. Dennis Croessman, 1520 |
| 1 | MS 0840 | John Pott, 1525 |
| 1 | MS 1323 | O. Erik Strack, 1443 |
| 1 | MS 0123 | D. Chavez, LDRD Office, 1011 |
| 1 | MS 0899 | Technical Library, 9536 (electronic) |

Sandia National Laboratories